Article

Iron Complexes Containing Electrochemically Active Diazocycle-bis(di-*tert*-butyl-phenol) Ligands

Luísa L. Mendes,[a,b] Christiane Fernandes,[a] Roberto W. A. Franco,[c] Leonardo M. Lube,[b] Sheng-Hsuan Wei,[d] Joseph H. Reibenspies,[d] Donald J. Darensbourg[d] and Adolfo Horn Jr.[a]*

[a]*Laboratório de Ciências Químicas, Universidade Estadual do Norte Fluminense Darcy Ribeiro, 28013-602 Campos dos Goytacazes-RJ, Brazil*

[b]*Instituto Federal Fluminense, 28030-130 Campos dos Goytacazes-RJ, Brazil*

[c]*Laboratório de Ciências Físicas, Universidade Estadual do Norte Fluminense Darcy Ribeiro, 28013-602 Campos dos Goytacazes-RJ, Brazil*

[d]*Department of Chemistry, Texas A&M University, 3255 TAMU, College Station, TX, USA*

Quatro ligantes *N,O*-doadores contendo unidades centrais diazocíclicas e grupos bis(di-*terc*-butilfenol) foram empregados na síntese de complexos de ferro(III), resultando em quatro complexos mononucleares e um binuclear. Os ligantes apresentados neste estudo diferem entre si na unidade diazocíclica, sendo elas: piperazina (H_2L1), diazepam/homopiperazina (H_2L2), hexaidropirimidina (H_2L3) ou hexaidropirimidin-5-ol (H_3L4). As estruturas moleculares dos complexos [FeL2Cl], **2**, e [Fe$_2$(L4)(HL4)Cl], **4**, foram elucidadas por difratometria de raios X de monocristal. Estudos eletroquímicos mostram que, além de processos redox centrados no metal, os complexos apresentam processos redox atribuídos aos ligantes. Estudos coulométricos acoplados a espectroscopia eletrônica no UV-Vis confirmam a formação da espécie radicalar para o complexo **2**, enquanto dados de espectroscopia de ressonância paramagnética eletrônica (EPR) mostram a formação do radical para os complexos **2**, **4** e **5**. De relevância é a observação de que o ligante que sofre oxidação em menor potencial eletroquímico é aquele cujo centro metálico apresenta a menor acidez de Lewis.

Four *N,O*-donor ligands built on diazocycle platforms and containing bis(di-*tert*-butyl-phenol) as pendant arms were employed in the synthesis of iron(III) complexes, resulting in four mononuclear and one dinuclear complexes. The ligands are distinct with respect to the diazocycle backbone: piperazine (H_2L1), diazepane/homopiperazine (H_2L2), hexahydropyrimidine (H_2L3) or hexahydropyrimidin-5-ol (H_3L4). The molecular structure of compounds [FeL2Cl], **2**, and [Fe$_2$(L4)(HL4)Cl], **4**, were solved by single crystal X-ray diffraction analysis. Electrochemical data showed that, in addition to the electrochemical process centered on the metal, the compounds show ligand-centered redox processes. Coulometric studies with concomitant UV-Vis analyses confirmed that compound **2** generated the phenoxyl species, while electron paramagnetic resonance (EPR) spectroscopy confirmed the radical formation for compounds **2**, **4** and **5**. Of interest was the observation that the compound in which the ligand can be oxidized easiest is the one where the metal center shows the lowest Lewis acidity.

Keywords: phenoxyl radical, iron compounds, diazocycle, *tert*-butylphenol, non-innocent ligand

*e-mail: adolfo@uenf.br

Introduction

The synthesis of coordination compounds employing redox active ligands has been considered of interest in several fields of inorganic chemistry, e.g., coordination chemistry,[1] catalysis,[2] and bioinorganic chemistry.[3] Examples of such ligands are α-diimines,[4,5] *tert*-butylphenol,[6-8] and porphyrins.[9] The presence of electrochemically active ligands has also been documented in natural systems. The highly oxidized intermediates observed in the catalytic cycle of P-450, heme-peroxidases and iron-catalase enzymes are described as containing the one electron oxidized porphinato anion, which results in iron(IV)-oxo porphyrin radical cation intermediates as the active species.[9-11] It is also very well known that phenoxyl radical is formed in the galactose oxidase catalytic cicle,[12,13] as well as it has been observed in ribonucleotide reductase.[9] As presented by Kaim,[14] the research involving redox active ligands poses several interests, including (*i*) the identification and the establishment of the non-innocent behavior; (*ii*) design and development of new ligands and their metal complexes; and (*iii*) their applications to organic/organometallic transformations.

Related to item (*ii*), there are some reports in the literature concerning the development of complexes containing two phenolate groups and two nitrogen atoms.[15] As exemplified by the work of Strautmann *et al.*,[16] the main goal in this area is to understand the electrochemical and spectroscopic features of these complexes. It has been shown that the redox processes observed in positive potential are ligand centered, resulting in phenoxyl radical species. Relevant to this subject, iron complexes containing tertiary diamines connected to 3,5-bis-*tert*-butylphenol have been characterized by spectroscopic, electrochemical and structural methods.[6,16,17] Among these iron complexes, just one of them contains a diazocyclic backbone (1,4-bis(2-hydroxy-3,5-di-*tert*-butylbenzyl)-1,4-diazepane).[17] The others were modeled on ethanediamine and *o*-phenylene diamine.[6,16]

Due to the restricted number of iron complexes containing diazocyclic units as central core and phenolate groups as pendant arms in the ligand structure, this work was designed to investigate the physical-chemical and structural features of iron complexes containing different diazocycle-bis(di-*tert*-butyl-phenol) ligands. Thus a family of diazocyclic ligand containing piperazine (H$_2$L1), homopiperazine/1,4-diazepane (H$_2$L2), hexahydropyrimidine (H$_2$L3) and hexahydropyrimidin-5-ol (H$_3$L4) (Figure 1) was prepared and the spectral (infrared (IR), UV-Vis, electron paramagnetic resonance (EPR)) and electrochemical characterization of their iron complexes were carried out. Furthermore, the molecular structure of the iron complexes containing H$_2$L2 and H$_3$L4 are presented. The radical species formed were confirmed by coulometry and monitored by EPR and UV-Vis (*in situ*) spectroscopies. In this study we have observed that the storage of oxidizing equivalents on the ligand was easiest in complexes with lower Lewis acidity.
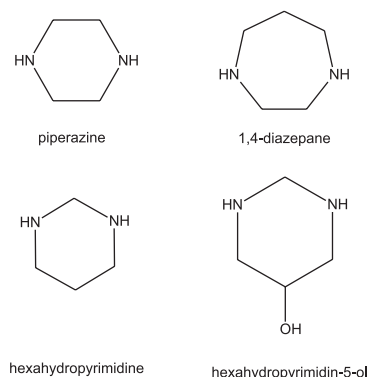
Figure 1. Diazocycle units employed in the synthesis of the ligands.

Experimental

Materials and general methods

All reagents and solvents for syntheses and analyses were of analytical and/or spectroscopic grade and used without further purification. Elemental (C, H, N) analysis was performed on a Thermo Scientific Flash 2000 CHN analyzer. Melting points were performed on a Fisatom melting point apparatus, model 430. Infrared spectra were recorded in KBr disks on a Shimadzu IRAffinity-1 and the electronic spectra (200-1100 nm range) were recorded in CH$_2$Cl$_2$ with a UV-Vis Cary 50 Bio Varian. The nuclear magnetic resonance (NMR) analyses were carried out in a Jeol Eclipse 400+ operating at 400 MHz for ^{1}H and 100 MHz for [13]C. Cyclic voltammograms (CVs) were carried out with an Autolab PGSTAT 10 potentiostat/galvanostat in dichlorometane containing 0.1 mol L^{-1} tetrabutylammonium perchlorate (TBAClO$_4$) as supporting electrolyte under an argon atmosphere at room temperature. The electrochemical cell employed was a standard three-electrode configuration with a platinum-wire as auxiliary electrode, a platinum wire as pseudo-reference electrode and a glassy carbon disk as the working electrode, for the complexes [FeL1]Cl (**1**), [FeL3]Cl (**3**) and [FeL4] (**5**). For complexes [FeL2Cl] (**2**) and [Fe$_2$(HL4)L4Cl] (**4**) a platinum disk was employed as working electrode. The ferrocenium/ferrocene redox couple was used as internal standard (0.400 V *vs.* normal hydrogen electrode (NHE)).[18] The potentials were corrected and are given *vs.* Fc/Fc$^+$. The electrochemical formation

of the phenoxyl radical species (bulk electrolysis) was carried out by using an Autolab PGSTAT 10 potentiostat/galvanostat in dichlorometane containing 0.1 mol L^{-1} tetrabutylammonium perchlorate (TBAClO$_4$) as supporting electrolyte under an argon atmosphere at 25 °C, and a three electrode system. The working electrode was a reticulated vitreous carbon electrode; the counter electrode and the pseudo-reference electrodes were platinum wires. Before the coulometry, cyclic voltammetry experiments were carried out to determine the potential range in which the ligand oxidation was taking place. Different potential were applied and spectral changes in the visible range were followed by *in situ* measurements employing a fiber optic probe connected to the Varian Cary 50 UV-Vis spectrophotometer. Samples of the solutions were frozen (liquid nitrogen) immediately before and after the electrochemical experiments and their EPR spectra were obtained at X-band frequency (9 GHz), at 100 K, using a Bruker E500 spectrometer with a high sensitive cylindrical cavity, and the following conditions: microwave power of 5 mW; modulation frequency of 100 kHz; modulation amplitude of 1 G. The Qpow program was used to simulate EPR spectra.[19] The g-factor was referenced by a MgO:Cr^{3+} (g = 1.9797) sample attached to the sample to be analyzed. The electrical conductivity of the complexes was measured with a Biocristal conductivity meter, in dichloromethane, employing a concentration of 1×10^{-3} mol L^{-1}.

The crystallographic analyses for complexes **2** and **4** were carried out with a Bruker GADDS diffractometer with graphite-monochromated Cu-K$_\alpha$ radiation at 110.15 K, using Olex2.[20] The structure was solved with the ShelXS[21] structure solution program using direct methods and refined with the ShelXL[22] refinement package using least squares minimization. All non-hydrogen atoms were refined anisotropically. H atoms attached to C atoms were placed at their idealized position, with C–H distances and U_{eq} values taken from the default settings of the refinement program. The H atom from the phenol group presented in **4** was found in the Fourier difference map and treated with a riding model. One of the *tert*-butyl groups observed in **4** was found to be disordered and was modeled with rigid bond restraints, with σ for 1-2 distances of 0.005 and σ for 1-3 distances of 0.005. A dark purple crystal of complex **2** with parallelogram form was isolated from a crystalline sample, while the crystals of complex **4** showed a dark red color, with needle shape. Both crystals were isolated from the reaction media after resting for a few days. Selected crystal and refinement data for both compounds are presented in Table 1, while selected bond lengths and angles are shown in Tables S1 and S2 as supplementary information.

Syntheses

The structure of the ligands and their iron(III) complexes are presented in Figure 2. The ligands H$_2$L1, H$_2$L2 and H$_2$L3 were synthesized as described previously and their characterizations are in agreement with the reported in the literature.[17,23-25]

H$_3$L4: This ligand was synthesized through the reaction between 2,4-di-*tert*-butylphenol (27.23 g, 0.132 mol), paraformaldehyde (3.96 g, 0.132 mol) and 1,3-diaminopropan-2-ol (3.0 g, 0.033 mol). The reagents were stirred for 120 h in methanol (120 cm^3) resulting in a yellow solution with a white solid. The precipitate was filtered, washed with methanol and dried under vacuum. Yield: 13.76 g (77%); m.p. 175-177 °C; elemental anal. calcd. for C$_{34}$H$_{54}$N$_2$O$_3$.½H$_2$O.½CH$_3$OH: C, 73.49; H, 10.19; N, 4.97; found: C, 73.26; H, 9.99; N, 4.54%; IR (KBr) ν$_{max}$/cm^{-1} 3603, 3391, 3000, 2955, 2905, 2870, 2812, 1481, 1442, 1236, 1204; ^{1}H NMR (CDCl$_3$, 400 MHz) δ 9.99 (s, 2H, OH), 7.25 (d, 2H, *J* 2.40 Hz, Ph–H), 6.87 (d, 2H, *J* 2.40 Hz, Ph–H), 4.04 (s, 1H, C<u>H</u>OH), 3.84 (d, 2H, *J* 13.5 Hz, NCH$_2$Ph), 3.77 (d, 2H, *J* 13.7 Hz, NCH$_2$Ph), 3.44 (s, 2H, NCH$_2$N), 2.89 (d, 2H, *J* 11.20 Hz, NC<u>H</u>$_2$CHOH), 2.61 (m, 2H, NC<u>H</u>$_2$CHOH), 1.43 (s, 18H, CH$_3$), 1.29 (s, 18H, CH$_3$); ^{13}C NMR (CDCl$_3$, 100 MHz) δ 29.6, 31.7, 34.2, 34.9, 57.1, 58.6, 63.0, 72.6, 119.9, 123.4, 123.7, 135.9, 140.9, 153.9; UV-Vis (CH$_2$Cl$_2$) λ$_{max}$/nm (ε/(L mol^{-1} cm^{-1})) 282 nm (4750), 285 nm (4770).

Complex [FeL1]Cl, **1**: To a solution of H$_2$L1 (0.26 g, 0.5 mmol, 20 cm^3 of dichloromethane) was added a solution of FeCl$_3$.6H$_2$O (0.24 g, 0.88 mmol, 15 cm^3 of methanol). The resulting brown solution was stirred for 10 min at room temperature. The solution was filtered, concentrated, and a new aliquot of dichloromethane was added. The purple solution was filtered and concentrated again, resulting in a purple solid. Yield: 0.27 g (89%); m.p. 163-164 °C; elemental anal. calcd. for C$_{34}$H$_{52}$N$_2$O$_2$ClFe.1/3CH$_3$OH: C, 58.32; H, 8.00; N, 3,83; found: C, 58.53; H, 8.00; N, 3.51%; IR (KBr) ν$_{max}$/cm^{-1} 3650-3350, 2951, 2904, 2866, 1481, 1460, 1234, 1204.

Complex [FeL2Cl], **2**: To a solution of H$_2$L2 (0.54 g, 1 mmol, 30 cm^3 of ethyl acetate) was added 0.27 g (1 mmol) of FeCl$_3$.6H$_2$O solubilized in 20 cm^3 of methanol. The resulting purple solution was stirred for 2 h at room temperature. After 2 days, a purple crystalline solid was formed and isolated by filtration. Yield: 0.29 g (46%); m.p. 291-293 °C; elemental anal. calcd. for C$_{35}$H$_{54}$ClFeN$_2$O$_2$: C, 67.14; H, 8.69; N, 4.47; found: C, 66.79; H, 9.21; N, 4.41%; IR (KBr) ν$_{max}$/cm^{-1} 2951, 2904, 2866, 1462, 1439, 1236, 1206.

Complex [FeL3]Cl, **3**: To a solution of H$_2$L3 (0.26 g, 0.5 mmol, 20 cm^3 of ethyl acetate) it was added 0.15 g

Table 1. Crystal data and structure refinement for complex **2** and **4**

Complex	2		4	
Empirical formula	$C_{35}H_{54}ClFeN_2O_2$		$C_{68}H_{103}ClFe_2N_4O_6$	
Formula weight	626.10		1219.69	
Temperature / K	110(2)		110(2)	
Wavelength / Å	1.54178		1.54178	
Crystal system	Orthorhombic		Triclinic	
Space group	P_n_a_21		P-1	
Unit cell dimensions	a = 11.8758(17) Å	α = 90°	a = 11.1121(17) Å	α = 74.155(9)°
	b = 29.192(4) Å	β = 90°	b = 17.975(3) Å	β = 73.098(8)°
	c = 10.0444(16) Å	γ = 90°	c = 18.250(3) Å	γ = 85.101(9)°
Volume / Å^3	3482.2(9)		3355.1(9)	
Z	4		2	
Density (calculated) / (Mg m^{-3})	1.194		1.207	
Absorption coefficient / mm^{-1}	4.408		4.229	
F(000)	1348		1312.0	
Crystal size / mm^3	$0.20 \times 0.20 \times 0.15$		$0.5 \times 0.02 \times 0.01$	
Theta range for data collection	4.02 to 119.72°		5.11 to 119.996°	
Index ranges	$-13 \leq h \leq 13, -32 \leq k \leq 32, -11 \leq l \leq 11$		$-12 \leq h \leq 12, -19 \leq k \leq 20, -20 \leq l \leq 19$	
Reflections collected	26177		20710	
Independent reflections	5033 [R(int) = 0.0733]		9192 [R(int) = 0.1059]	
Absorption correction	multi-scan		multi-scan	
Max. and min. transmission	0.5577 and 0.4726		0.4608 and 0.2912	
Refinement method	Full-matrix least-squares on F^2		Full-matrix least-squares on F^2	
Data / restraints / parameters	5033 / 1 / 382		9192 / 192 / 760	
Goodness-of-fit on F^2	1.001		1.037	
Final R indices [I > 2σ(I)]	$R_1 = 0.0369$, $wR_2 = 0.0780$		$R_1 = 0.0984$, $wR_2 = 0.2058$	
R indices (all data)	$R_1 = 0.0473$, $wR_2 = 0.0817$		$R_1 = 0.1381$, $wR_2 = 0.2286$	
Largest diff. peak and hole	0.281 and −0.462 e Å^{-3}		0.99 and −0.49 e Å^{-3}	
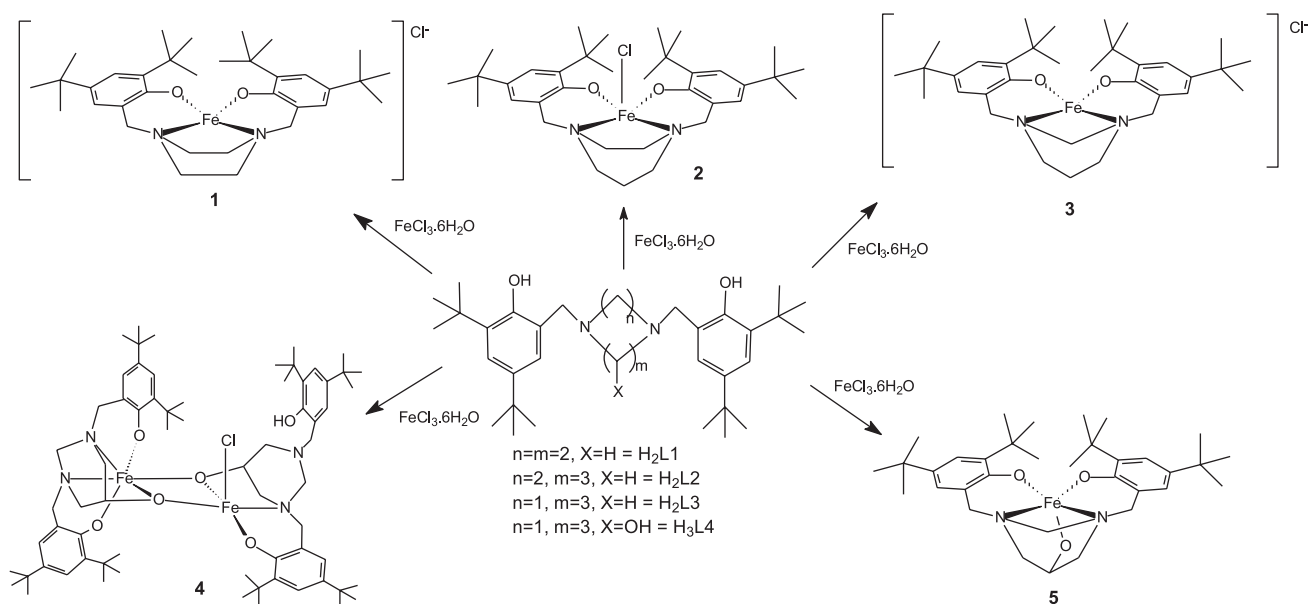
Figure 2. Scheme for the synthesis of complexes **1**-**5**.

(0.56 mmol) of $FeCl_3.6H_2O$ dissolved in 20 cm^3 of methanol. The resulting purple solution was stirred for 20 min at room temperature. The solution was filtered and concentrated under vacuum. Dichloromethane was then added and the purple solution was filtered and concentrated again, resulting in a deep purple solid. Yield: 0.22 g (71%); m.p. 129-131 °C; elemental anal. calcd. for $C_{34}H_{52}ClFeN_2O_2.3/2CH_3OH.3/2H_2O$: C, 62.05; H, 8.95; N, 4.08; found: C, 61.97; H, 8.53; N, 4.08%; IR (KBr) ν_{max}/cm^{-1} 3194, 2959, 2907, 2868, 1481, 1462, 1233, 1204.

Complex [Fe₂(HL4)L4Cl], **4**: To a solution of H_3L4 (0.54 g, 1 mmol, 30 cm^3 of ethyl acetate) was added a solution of $FeCl_3.6H_2O$ (0.27 g, 1 mmol, 20 cm^3 of methanol). The resulting purple solution was stirred for 1 h at room temperature. After 5 days a purple crystalline solid was formed and isolated by filtration. Yield: 0.046 g (14%); m.p. > 300 °C; elemental anal. calcd. for $C_{68}H_{103}ClFe_2N_4O_6$: C, 66.96; H, 8.51; N, 4.59; found: C, 65.87; H, 8.91; N, 4.53%; IR (KBr) ν_{max}/cm^{-1} 3449, 2961, 2905, 2868, 1466, 1439, 1240, 1204.

Complex [FeL4], **5**: To a solution of H_3L4 (0.54 g, 1 mmol, 30 cm^3 of ethyl acetate), 0.27 g (1 mmol) of $FeCl_3.6H_2O$ in 20 cm^3 of methanol was added, followed by the addition of triethylamine (0.81 g, 8 mmol), resulting in a red solution which was stirred for 1 h at room temperature. After 1 day, a needle-shaped red microcrystalline solid was formed and isolated by filtration. Yield: 0.22 g (37%); m.p. > 300 °C; elemental anal. calcd. for $C_{34}H_{51}FeN_2O_3$. $CH_3OH.H_2O$: C, 65.51; H, 8.95; N, 4.37; found: C, 65.20; H, 8.93; N, 4.12%; IR (KBr) ν_{max}/cm^{-1} 2953, 2903, 2866, 1470, 1441, 1240, 1202.

Results and Discussion

Synthesis and general characterization

The four ligands presented in this report were prepared with the aim of synthesizing iron complexes containing an unsaturated coordination environment. This feature makes the complexes of interest for future studies as catalyst, since an open/labile coordination site is generally observed in the active site of metalloenzymes.[26-29] Furthermore, the presence of coordination site on the metal is of importance in catalytic reaction, since it allows small molecules like O_2, H_2O, CO_2, etc., to bind to the metal center for activation.[30-34] An added goal of this study is to evaluate the influence of the ring size, as well as the position of the nitrogen atoms, in the diazocyclic unit on the physical-chemical and structural properties of the iron(III) center. Thus, the ligands H_2L1, H_2L3 and H_3L4 possess a six-membered diazocycle ring, whose difference is in the position of the nitrogen atom in

the cycle: positions 1,4 for H_2L1, 1,3 for H_2L3 and H_3L4. The two latter are distinct due to the presence, in H_3L4, of an alcohol group bound to the central carbon atom located in the propanediamine backbone. On the other hand, the ligand H_2L2 contains a seven-member ring, whose nitrogen atoms are at the 1,4 positions.

From the four ligands employed in this study, three of those were previously published in the literature.[17,23-25] H_3L4 is a new ligand and it was obtained using the same methodology employed in the synthesis of H_2L3. Ligands H_2L2, H_2L3 and H_3L4 formed iron complexes that are very stable in the solid state, as well as in solution. On the other hand, the isolation of the complex containing the ligand H_2L1 was very difficult. Its complex, **1**, is very unstable in protic solvent, as was observed by the fast loss of its deep purple color in alcohol solution. The same behavior is observed in CH_3CN, DMSO, ethyl acetate and acetone. A longer stability was achieved in CH_2Cl_2. Although there is in the literature some iron complexes containing a six membered diazocyclic unit (piperazine),[35] this work reveals that six-membered 1,4-diazocyclic ligand containing phenol groups as pendant arms are less stable than those containing nitrogen atoms at the 1,3 positions (H_2L3 and H_3L4) or than the seven-membered diazocyclic backbone (H_2L2). The synthesis, UV-Vis and electrochemical characterization of **2** were described previously,[17] but no structural data was available at that time.

### X-ray molecular structures for complexes **2** and **4**

The molecular structure of **2** is shown in Figure 3. The iron center is pentacoordinated, showing an almost perfect square pyramidal geometry ($\tau = 0.06$; $[\tau = (\beta - \alpha) / 60]$),[36] with the ligand adopting a trans conformation. The basal plane is formed by oxygen and nitrogen atoms from the ligand, while the axial position is occupied by the chloro ligand. The iron(III) ion is 0.521 Å above the basal plane. The respective bond lengths are: Fe1−O1 = 1.868(2), Fe1−O2 = 1.865(2), Fe1−N1 = 2.177(3), Fe1−N2 = 2.186(2), and Fe1−Cl1 = 2.251(1) Å, being similar to those reported for a related complex Fe(L)Cl ($H_2L = N,N'$-dimethyl-N,N'-bis-(3,5-di-*t*-butyl-2-hydroxybenzyl)-1,2-diaminoethane), which contains an acyclic diamine.[6] However, in this latter compound, the two Fe–N distances are different, (Fe–N8 = 2,163(3) and Fe–N11 = 2.284(3) Å), while in **2** they are very similar. This different behavior concerning the coordination of the diamine unit may be explained by the presence of the diazocyclic ring in **2**, which makes the structure less flexible than that present in the Fe(L)Cl complex containing the ethanediamine backbone.

When the similar ligand 1,4-bis-(2-hydroxybenzyl)-1,4-diazepane (a ligand similar to H₂L2, but without the *tert*-butyl groups) reacted with FeCl₃, a dinuclear μ-oxo complex was obtained and characterized by X-ray diffraction.[17] The metal-ligand bond distances are similar to those observed in **2**. The presence of *tert*-butyl groups is most likely responsible for the lack of dimer formation in this instance.
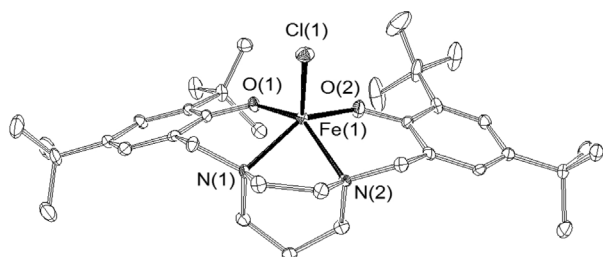
Figure 3. A perspective view of molecular structure of **2** with atomic labeling. The ellipsoids are shown with 50% probability level. Hydrogen atoms have been omitted for clarity.

Compound **4** shows an unsymmetrical dinuclear structure (Figure 4). It contains two molecules of the ligand H₃L4, two iron(III) centers and one chloro ligand. The iron(III) ions (Fe1···Fe2 = 3.195 Å) are connected through two alkoxide bridges (O3, O4), which come from the ligands. The metal centers present different coordination arrangements. Fe1 is six-coordinate while Fe2 is five-coordinate. The ligand molecule around Fe1 is coordinated by all of its donor atoms (N₂O₃). In contrast, the ligand bonded to Fe2 displays a NO₂ coordination set, leaving
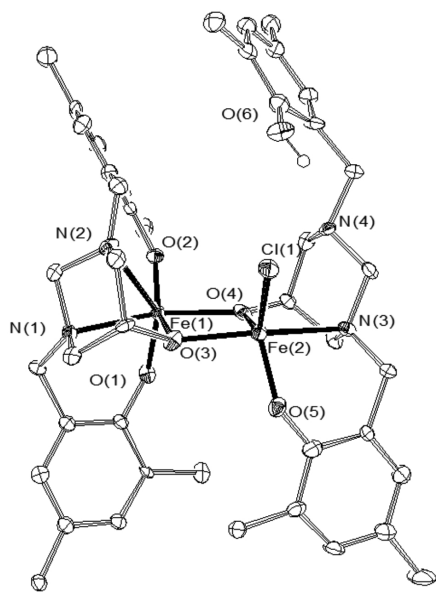
an amine (N4) and a phenol (O6) groups away from the iron center. There is a chloro ligand completing the Fe2 coordination sphere.

For Fe1, the equatorial plane is formed by two oxygen atom (O1 and O4), and also by two nitrogen atoms (N1 and N2). This iron center exhibits a distorted octahedral geometry. The respective bond lengths are: Fe1−O1 = 1.900(7), Fe1−O2 = 1.867(8), Fe1−O3 = 2.055(7), Fe1−O4 = 2.022(8), Fe1−N1 = 2.25(1), Fe1−N2 = 2.295(7) Å. Surprisingly, there is a very small coordination angle connecting N1–Fe1–N2 atoms, 60.0(3)°, which is, to the best of our knowledge, the smallest one already reported in the literature for a N–Fe–N angle.[37-41] This small angle is the result of a 4-membered ring containing the Fe1–N1–C16–N2 atoms. For comparison, the angle N–Fe–N (six-membered ring) observed in **2** is 72.60(1)°.

The Fe2 center has a distorted square pyramidal geometry (τ = 0.413).[36] The respective bond lengths are: Fe2−O3 = 1.993(8), Fe2−O4 = 1.9959(7), Fe2−O5 = 1.839(7), Fe2−N3 = 2.23(1), Fe2−Cl1 = 2.254(3) Å. The bond length of Fe2−O5 [1.839(7) Å] is very similar to that observed in compound **2** [Fe1−O1 = 1.868(2) and Fe1−O2 = 1.865(2) Å], but the connections with oxygen alkoxide are slightly longer [Fe2−O3 = 1.993(8) and Fe2−O4 = 1.959(7) Å]. The bond Fe2−N3 (2.23(1) Å) is a bit longer than those observed in compound **2** [Fe1−N1 = 2.177(3) and Fe1−N2 = 2.186(2) Å], probably due to the steric hindrance.

Infrared and electronic spectroscopies

The infrared spectra of the ligands are very similar. All of them display the bands typical of aromatic ring (1450-1480 cm⁻¹), the C–O stretching characteristic of phenol group (1235 cm⁻¹) and a broad band centered about 3000 cm⁻¹, attributed to O–H group making hydrogen bonds. In this same range, it is possible to observe some peaks attributed to the methyl and methylene groups. Upon complexation, the broad band disappears, with narrow bands remaining, which confirm the presence of *tert*-butyl groups and methylene units as well. Above 3200 cm⁻¹, compounds **1** and **3** present a broad band typical of O–H stretching, which may be due to the presence of solvent molecules as observed in the elemental analysis. On the other hand, this region has no bands for compounds **2** and **5**, while for compound **4**, there is a very narrow strong band, which is typical of O–H group lacking hydrogen bonding, as that observed in the X-ray molecular structure. The position of the C–O stretching vibration does not change significantly after complexation.

Figure 4. A perspective view of molecular structure of **4** with atomic labeling. The ellipsoids are shown with 50% probability level. Hydrogen atoms and *tert*-butyl groups have been omitted for clarity.

The electronic spectra were obtained in dichloromethane. The spectra of the ligands show similar features: a broad band centered at 283 nm that is clearly composed of two overlapping bands whose maxima can be observed near 280 and 285 nm, which are attributed to intraligand $\pi \rightarrow \pi*$ transitions. The ε values are close to 4.6×10^3 L mol^{-1} cm^{-1} for the ligands H_2L1, H_2L2 and H_3L4, and 6.3×10^3 L mol^{-1} cm^{-1} for H_2L3. The spectra of **1** and **3** show four bands, whereas the spectra of **2**, **4** and **5** present 3 bands between 250-1100 nm. The most intense bands observed are between 240-320 nm, which are typical of intraligand charge transfer $\pi \rightarrow \pi*$ (Table 2). The bands observed in the range 330-360 nm are assignable as ligand to metal charge transfer (LMCT) phenolate $p\pi \rightarrow Fe^{III} d\sigma*$. The less intense bands, which are observed in the range 480-550 nm, are assignable to (LMCT) phenolate $p\pi \rightarrow Fe^{III} d\pi*$.[6,7,16,17] This transition accounts for the purple color observed for **1**, **2** and **3**, the pink color for **4** and the red one for **5**. It is intriguing that compounds **1** and **3** show a different number of bands (four bands) in the UV-Vis spectra when compared with compounds **2**, **4**, and **5** (three bands). In the electronic characterization of the compounds, FeLCl and FeLNO$_3$,[6] which exhibit five and six-coordination geometries, it was also observed only 3 bands in dichloromethane solution. Theoretical calculations of these compounds (FeLCl and FeLNO$_3$) supported that the two bands of lower energies are LMCT, and the bands at higher energy are intraligand transitions.[6] Thus, the difference in the number of bands observed in the electronic

spectra of the compounds suggests that the coordination environment and the geometry for **1** and **3** should be distinct from **2**, **4** and **5**. Another interesting point is that the ε value for the band at lowest energy observed for **1**, **3**, and **5** are much lower (< 1000 L mol^{-1} cm^{-1}) when compared with the band observed for **2** and **4** and for the compound FeLCl (5400 L mol^{-1} cm^{-1}).[6] This suggests that the overlap between the phenolate $p\pi$ and iron(III) $d\pi$ are very poor for the formers, probably due to steric hindrance. On the other hand, we can assume that the overlap involving the orbital phenolate $p\pi$ and iron(III) $d\sigma$ are very effective, as the ε values of the bands that involve these orbitals demonstrate.

Electrochemistry

Cyclic voltammetry and conductimetry were employed in the electrochemical characterization of the complexes (Table 2 and Figure 5). Conductimetric analyses showed that complexes **2**, **4** and **5** are neutral species in CH_2Cl_2 solution, while compound **3** shows a conductivity measure in the range of 1:1 electrolyte type.[42] Complex **1** showed a value between neutral and 1:1 species, but, based on the cyclic voltammetry data (see below) we are proposing that it is a 1:1 species.

The cyclic voltammetry of all the complexes showed redox process attributed to the metal center (Figure 5, processes E^1 and $E^{1'}$). The voltammograms for complexes **1**, **2**, **3** and **5** are typical of mononuclear complexes, since they show only one redox metal-centered process in the range

Table 2. UV-Vis and electrochemical[a] data for complexes **1**, **2**, **3**, **4** and **5** in dichloromethane

Complex	[FeL1Cl] **1**	[FeL2Cl] **2**	[FeL3]Cl **3**	[Fe$_2$(HL4)L4Cl] **4**	[FeL4] **5**
λ_{max} / nm (ε / (L mol^{-1} cm^{-1}))	282(5770) 317(3890) 360(3200) 540(702)	281(13300) 342(8530) 550(6730)	280(6660) 316(4700) 360(3160) 540(579)	282(34200) 332(19300) 514(8980)	282(2740) 331(1760) 489(797)
Ω / (μS cm^{-1})	7.8	0.0	12.7	0.5	0.0
E^1_{pa} / mV	−365	−1048	−349	−992	−1598
$E^{1'}_{pa}$ / mV	–	–	–	−1533	–
E^1_{pc} / mV	−515	−1397	−599	−1112	−1748
$E^{1'}_{pc}$ / mV	–	–	–	−1744	–
$E^1_{1/2}$ / mV	−440	−1222	−474	−1052	−1673
$E^{1'}_{1/2}$ / mV	–	–	–	−1638	–
E^2_{pa} / mV	783	798	998	540	406
E^2_{pc} / mV	–	399	–	360	295
$E^2_{1/2}$ / mV	–	598	–	450	350
E^3_{pa} / mV	–	1148	–	–	606
E^3_{pc} / mV	–	798	–	721	491
$E^3_{1/2}$ / mV	–	973	–	–	548

[a]Electrochemical potentials are given *vs.* Fc/Fc$^+$.
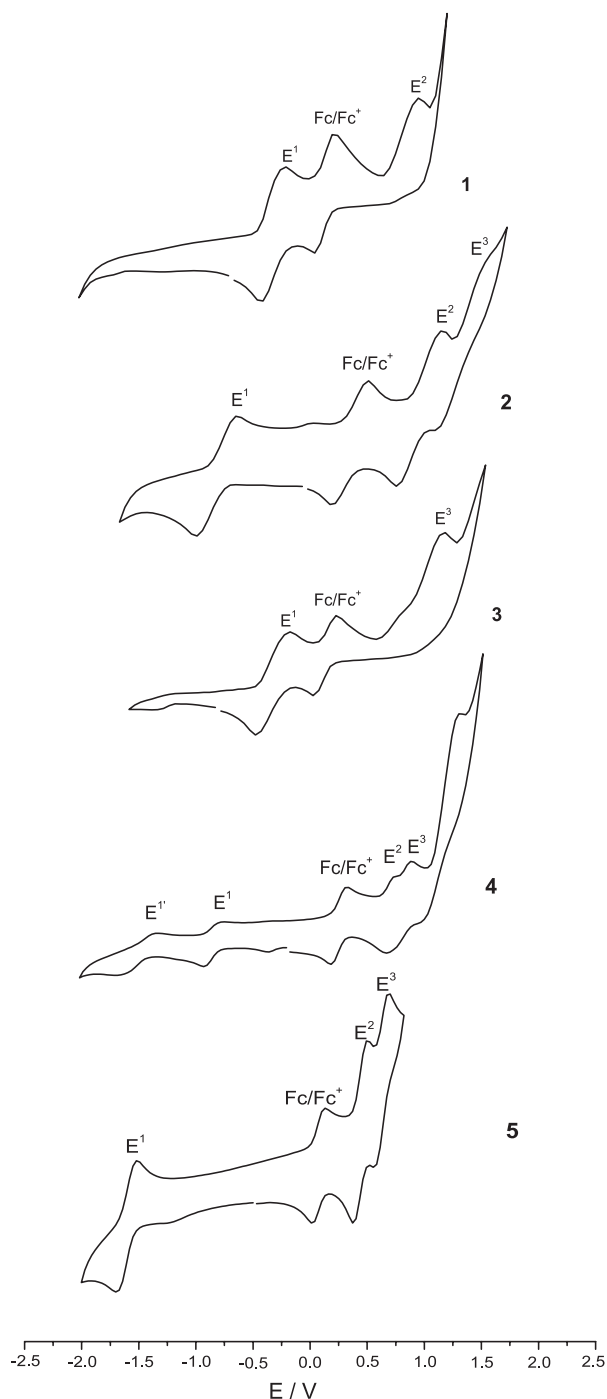
Figure 5. Cyclic voltammograms in dichloromethane of complexes **1**, **2**, **3**, **4** and **5**. E^1 and $E^{1'}$ represent redox processes centered on the iron centers, while E^2 and E^3 indicate redox processes centered on the ligand. Fc/Fc$^+$ = ferrocene/ferrocenium redox couple.

of −2.0 to 0.3 V. This is in agreement with other analyses, including the X-ray diffraction data for complex **2**, which also confirms the formation of mononuclear complex. On the other hand, the cyclic voltammetry for complex **4** shows two redox processes (E^1 and $E^{1'}$) at negative potential range, which is characteristic of a dinuclear complex and is in accordance with the X-ray molecular structure. The

$E_{1/2}$ for the mononuclear complexes decreases in the order **1** ≈ **3** > **2** > **5**, which means that complexes **1** and **3** show the most acidic iron(III) centers in this series. Complex **2** presents a redox potential that is about 780 mV more negative than that from complex **1**. Since the conductivimetric study for complex **1** suggests that the chloride ion is acting as a counter ion in **1**, the difference in the redox potential between these two complexes may be ascribed to the presence of the chloro ligand bonded to the iron ion in **2** (as confirmed by X-ray analysis) and its absence in **1**, since the coordination of the chloro ligand decreases the Lewis acidity of the iron center. This also supports the fact that compound **1** show the most acidic iron center in this series.

Interestingly, it was observed that the iron center in **3** shows a redox potential very similar to that observed in **1**, which suggests that the coordination environment of the iron centers in both complexes should be similar (N_2O_2), and supports the claim that these complexes should be 1:1 electrolyte type, where the chloride species is acting as counterion and not as ligand.

On the other hand, the voltammogram observed for complex **4** indicates that the coordination environment around the iron centers is kept in the mixed valence as well as in the totally reduced species, since both redox couples ($Fe^{III}_2/Fe^{III}Fe^{II}$ and $Fe^{III}Fe^{II}/Fe^{II}_2$) showed a *quasi*-reversible electrochemical behavior. Complex **5** presents the least acid iron(III) center, reflecting the presence of the alcohol group in the ligand structure and its coordination as alkoxide to the metal ion.

When the electrochemical analyses were conducted above 0.5 V, redox processes (E^2, E^3) attributed to the oxidation of the ligand (di-*tert*-butylphenolate*)* were observed for all the complexes. Similar observations have been described previously in other compounds containing *tert*-butylphenol ligands, being ascribed as the oxidation of this unit and the generation of phenoxyl radical.[6-8,16]

Compounds **1** and **3** showed just one irreversible oxidative process at 783 and 998 mV, respectively. Above these potential we have observed a constant increase of the current (data not shown) without any other defined oxidation wave. Wieghardt and co-workers have proposed that the lack of reversibility of these processes indicates that a chemical reaction (polymerization) can be induced by the electrochemical process, resulting in the extinction of the radical species.[43] This similar behavior also supports that the coordination environment around the metal center in **1** and **3** should be similar as mentioned above. On the other hand, compound **2** showed two *quasi*-reversible oxidative processes centered on the ligand, indicating the formation of the species [FeL2Cl]$^+$ and [FeL2Cl]$^{2+}$. The dinuclear compound **4** showed two close oxidation waves and just

one broad reduction process at positive range. It is possible that this reductive wave is composed of two electron reduction. Compound **5** exhibited two well-defined redox processes and their redox potential are the lowest of the set of compounds described in this study. These observations may be explained by the fact that **5** represents the least acidic iron center and that, due to this, the electron density is preferentially localized on the aromatic rings which makes easier to carry out their oxidation.

Radical species formation and characterization

Due to the redox processes observed at positive potential, bulk electrolysis were carried out aiming to confirm if at these potential, a radical species would be formed. The experiments were followed by *in situ* UV-Vis spectroscopy as well as by EPR. Figure 6 shows the spectral changes in the UV-Vis spectra of the complexes **2**, **4** and **5** during the bulk electrolysis. Only for complex **2** it was possible to follow a significant change in the spectrum during electrolysis. The band at 552 nm decreased and a new band near 420 nm appeared, which is typical of phenoxyl radical[6,7,16] as described previously. For complexes **4** and **5**, the spectra do not change significantly, but it was possible to observe a small tendency to form a new band close to 420 nm. On the other hand, no change was observed in the spectra of complexes **1** and **3** after electrolysis. It is important to point out that usually this phenoxyl radical UV-Vis absorption is clearly detected at low temperature[6,16] due to the high reactivity of these species, and this may explain why it was not possible to observe clearly this band for compounds **1**, **3**, **4** and **5**. However, for compound **2**, this spectral signature could be characterized at 25 $^{\circ}$C, indicating the high stability of the radical species formed.

In an attempt to confirm the formation of phenoxyl radical species in compounds **1**, **3**, **4** and **5**, EPR spectra (100 K) were taken before and immediately after electrolysis (Figure 7). In all spectra, we observed lines characteristic of iron(III) in octahedral site at g = 2, and in orthorhombic site at g = 4. After electrolysis, an intense and isotropic signal, with Gaussian line shape and linewidth 1.3 mT, is observed at g = 2.0045 for complexes **2**, **4** and **5**. The parameters of this line is consistent with the presence of phenoxyl radical species.[6,16]

As observed in *in situ* UV-Vis experiments, EPR spectroscopy also could not detect the presence of radical species for complexes **1** and **3** after electrolysis, although the cyclic voltammetry study had shown that these complexes present related electrochemical processes involving ligand oxidation. This lack of detectable radical signature indicates that the radical species formed after
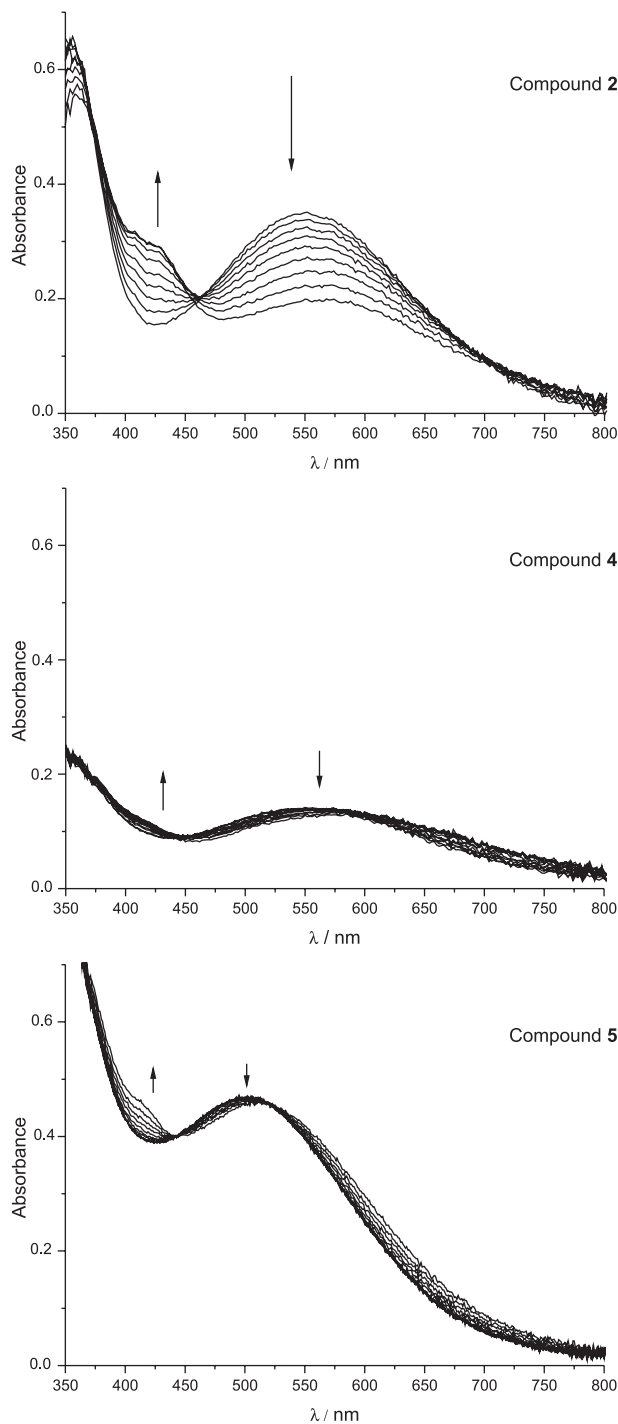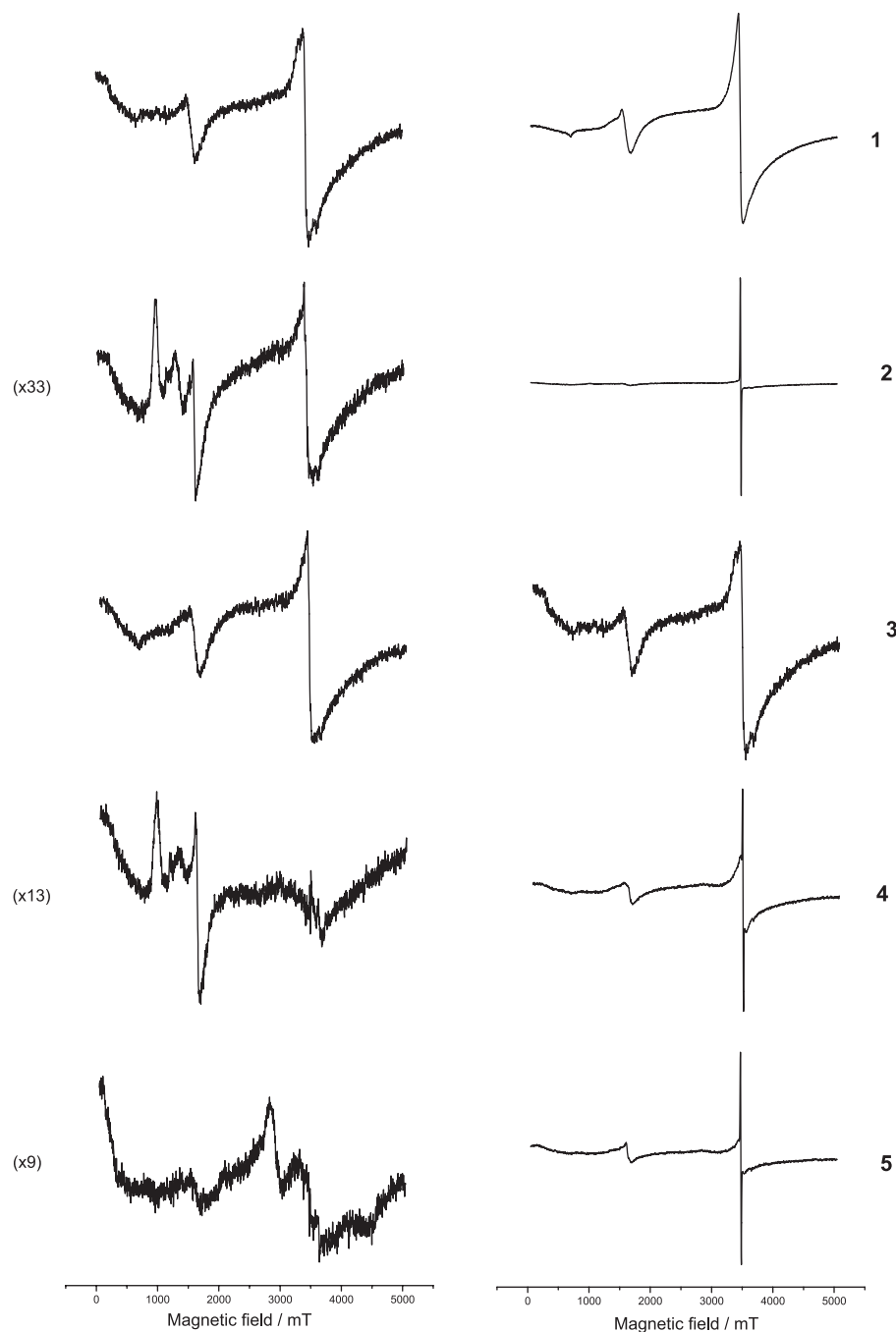
Figure 6. UV-Vis spectra obtained during bulk electrolysis of compounds **2** (top), **4** (middle) and **5** (bottom).

compounds **1** and **3** oxidation undergo a fast chemical reaction, resulting in the extinction of phenoxyl radical.

Conclusions

This work clearly reveals that the diazocyclic units employed in this study were able to coordinate to iron(III)

Figure 7. EPR spectra of the complexes **1** to **5** measured in CH_2Cl_2 (100 K) before (left) and after (right) electrolysis. Some spectra before electrolysis were enlarged by the factor shown in parentheses.

salts, resulting in complexes with free coordination site. However, complex **1**, which was synthesized with the piperazine backbone (1,4-diazocyclohexane) ligand shows lower stability when compared with others whose nitrogen atoms are at 1,3 position (H_2L3 and H_3L4) or 1,4-diazocycloheptane. Of interest also is the fact that the chemical analyses indicate that both ligand H_2L1 and H_2L3, which have similar ring sizes (six-membered), but with the nitrogen atoms at different positions (1,4 *vs.* 1,3), form iron

compounds with similar spectroscopic and electrochemical features, implying similar structures of the iron complexes. Our results indicate that the presence of the alcohol group in H_3L4 is of importance when designing ligands containing redox active groups, since its coordination as alkoxide decreased the Lewis acidity of the metal center and aids in the oxidation of the phenolate groups as observed by the electrochemical potential presented by complex **5**. However, the complex which shows the most stable radical

species is complex **2**, whose ligand contains a 7-member diazocycle ring and whose phenoxyl radical could be detected at 25 ºC by UV-Vis spectroscopy. Furthermore, our data shows that the electrochemical potential to store one oxidizing equivalent on the ligand's structure may be tuned by changing the diazocycle ring and by the presence of good donor groups on the ligand structure. Studies are being carried out at the moment to evaluate if this same behavior is observed with other metal compounds and will be the subject of a future publication.

Supplementary Information

Supplementary data (tables containing selected bond lengths and angles for complexes **2** and **4**, ^{1}H, ^{13}C NMR, IR and UV-Vis data) are available free of charge at http://jbcs. sbq.org.br as PDF file. Crystallographic data (excluding structure factors) for the structures in this work were deposited at the Cambridge Crystallographic Data Centre as supplementary publication numbers CCDC 973123 and 972966. Copies of the data can be obtained, free of charge, via www.ccdc.cam.ac.uk/conts/retrieving.html or from the Cambridge Crystallographic Data Centre, CCDC, 12 Union Road, Cambridge CB2 1EZ, UK; fax: +44 1223 336033; e-mail: deposit@ccdc.cam.ac.uk.

Acknowledgments

References

1. Shimazaki, Y.; Yamauchi, O.; *Indian J. Chem., Sect. A* **2011**, *50A,* 383.

2. Blanchard, S.; Derat, E.; Murr, M. D.; Fensterbank, L.; Malacria, M.; Mansuy, V. M.; *Eur. J. Inorg. Chem.* **2012**, 376.

3. Kaim, W.; Schwederski, B.; *Coord. Chem. Rev.* **2010**, *254*, 1580.

4. Chirik, P. J.; Wieghardt, K.; *Science* **2010**, *327*, 794.

5. Kaim, W.; Sieger, M.; Greulich, S.; Sarkar, B.; Fiedler, J.; Zális, S.; *J. Organomet. Chem.* **2010**, *695*, 1052.

6. Strautmann, J. B. H.; George, S. D.; Bothe, E.; Bill, E.; Weyhermüller, T.; Stammler, A.; Bögge, H.; Glaser, T.; *Inorg. Chem.* **2008**, *47*, 6804.

7. Anjos, A.; Bortoluzzi, A. J.; Caro, M. S. B.; Peralta, R. A.; Friedermann, G. R.; Mangrich, A. S.; Neves, A.; *J. Braz. Chem. Soc.* **2006**, *17,* 1540.

8. Chaudhuri, P.; Wieghardt, K.; *Prog. Inorg. Chem.* **2001**, *50*, 151.

9. Pan, Z.; Zhang, R.; Newcomb, M.; *J. Inorg. Biochem.* **2006**, *100*, 524.

10. Ghosh, A.; Steene, E.; *J. Biol. Inorg. Chem.* **2001**, *6*, 739.

11. Hessenauer-Ilicheva, N.; Franke, A.; Meyer, D.; Wogon, W. D.; Eldik, R.; *Chem. Eur. J.* **2009**, *15*, 2941.

12. Whittaker, M. M.; Whittaker, J. W.; *J. Biol. Chem.* **1990**, *265*, 9610.

13. Ito, N.; Phillips, S. E. V.; Stevens, C.; Ogel, Z. B.; Mcpherson, M. J.; Keen, J. N.; Yadav, K. D. S.; Knowles, P. F.; *Nature* **1991**, *350*, 87.

14. Kaim, W.; *Inorg. Chem.* **2011**, *50*, 9752.

15. Lyons, C. T.; Stack, T. D. P.; *Coord. Chem. Rev.* **2013**, *257,* 528.

16. Strautmann, J. B. H.; Richthofen, C. G. F.; Brückner, G. H.; DeBeer, S.; Bothe, E.; Bill, E.; Weyhermüller, T.; Stamller, A.; Bögge, H.; Glaser, T.; *Inorg. Chem.* **2011**, *50,* 155.

17. Mayilmurugan, R.; Stoeckli-Evans, H.; Suresh, E.; Palaniandavar, M.; *Dalton Trans.* **2009**, 5101.

18. Gagne, R. R.; Koval, C. A.; Lisensky, G. C.; *Inorg. Chem.* **1980**, *19*, 2854.

19. Nilges, M. J.; Matterson, K.; Belford, R. L. In *ESR Spectroscopy in Membrane Biophysics: Biological Magnetic Resonance*; Hemminga, M. A.; Berliner, L. J., eds.; Springer Verlag: New York, USA, 2007, Appendix 2.

20. Dolomanov, O. V.; Bourhis, L. J.; Gildea, R. J.; Howard, J. A. K.; Puschmann, H.; *J. Appl. Crystallogr.* **2009,** *42*, 339.

21. Sheldrick, G. M.; SHELXS-97; Program for Crystal Structure Refinement; University of Göttingen, Germany, 1990.

22. Sheldrick, G. M.; *Acta Crystallogr., Sect. A: Found. Crystallogr.* **2008**, *64*, 112.

23. Mohanty, S.; Suresh, D.; Balakrishna, M. S.; Mague, J. T.; *Tetrahedron* **2008**, *64,* 240.

24. Farwell, J. D.; Hitchcock, P. B.; Lappert, M. F.; Luinstra, G. A.; Protchenko, A. V.; Wei, X.-H.; *J. Organomet. Chem.* **2008**, *693*, 1861.

25. Farrell, J. R.; Niconchuk, J.; Higham, C. S.; Bergeron, B. W.; *Tetrahedron Lett.* **2007**, *48*, 8034.

26. Hrycay, E. G.; Bandiera, S. M.; *Arch. Biochem. Biophys.* **2012**, *522*, 71.

27. Rosenzweig, A. C.; Frederick, C. A.; Lippard, S. J.; Nordlund, P.; *Nature* **1993**, *366*, 537.

28. Gerdemann, C.; Eicken, C.; Krebs, B.; *Acc. Chem. Res.* **2002**, *35,* 183.

29. Bugg, T. D. H.; *Tetrahedron* **2003**, *59,* 7075.

30. Friedle, S.; Reisner, E.; Lippard, S. J.; *Chem. Soc. Rev.* **2010**, *39,* 2768.

31. Sun, C. L.; Li, B. J.; Shi, Z. J.; *Chem. Rev.* **2011**, *111,* 1293.

32. Lu, X.; Darensbourg, D. J.; *Chem. Soc. Rev.* **2012**, *41,* 1462.

33. Darensbourg, D. J.; *Inorg. Chem.* **2010**, *49,* 10765.

34. Darensbourg, D. J.; *Chem. Rev.* **2007**, *107,* 2388.

35. Caovilla, M.; Caovilla, A.; Pergher, S. B. C.; Esmelindro, M. C.; Fernandes, C.; Dariva, C.; Bernardo-Gusmão, K.; Oestreicher, E. G.; Antunes, O. A. C.; *Catal. Today* **2008**, *133-135,* 695.

36. Addison, A. W.; Rao, T. N.; Reedijk, J.; Rijn, J.; Verschoor, G. C.; *J. Chem. Soc., Dalton Trans.* **1984**, 1349.

37. Kabir, S. M. L.; Ruf, M.; Vahrenkamp, H.; *J. Organomet. Chem.* **1998**, *571,* 91.

38. Handley, D. A.; Hitchcook, P. B.; Lee, T. H.; Leigh, G. J.; *Inorg. Chim. Acta* **2001**, *314,* 14.

39. Mathur, P.; Singh, A. K.; Mohanty, J. R.; Chatterjee, S.; Mobin, S. M.; *Organometallics* **2008**, *27,* 5094.

40. Doedens, R. J.; *Inorg. Chem.* **1968**, *7,* 2323.

41. Foley, S. R.; Yap, G. P. A.; Richeson, D. S.; *Inorg. Chem.* **2002**, *41,* 4149.

42. Geary, W. J.; *Coord. Chem. Rev.* **1971**, *7,* 81.

43. Kimura, S.; Bill, E.; Bothe, E.; Weyhermüller, T.; Wieghardt, K.; *J. Am. Chem. Soc.* **2001**, *123,* 6025.